[20] Goulard, R., "Fundamental equations of radiation gas dynamics," AGARD Fluid Dynamics Panel Meeting, High Temperature Aspects of Hypersonic Flow, Rhode Saint Genese, Belgium (April 1952).
[21] Bohm, D., *Quantum Theory* (Prentice-Hall, Inc., New York, 1951), Chap. 10.
[22] Bates, D. R. (ed.), *Atomic and Molecular Processes* (Academic Press, New York, 1962), Chap. 3.
[23] Weissler, G. L., *Handbuch der Physik* (Springer-Verlag, Berlin, 1956), Vol. XXI, pp. 304–342.
[24] Pipkin, A. C., "Precursor waves in shock tubes," Phys. Fluids 6, 1382–1388 (1963).
[25] Langmuir, I., "The effect of space charge and initial velocities on the potential distribution and thermionic current between parallel plane electrodes," Phys. Rev. 21, 419–435 (1923).

JULY 1964 AIAA JOURNAL VOL. 2, NO. 7

A Quasi-One-Dimensional Treatment of Chemical Reactions in Turbulent Wakes of Hypersonic Objects

S. C. LIN* AND J. E. HAYES†
Avco-Everett Research Laboratory, Everett, Mass.

The effects of different mixing models on the chemical reaction histories in the turbulent wakes of hypersonic objects are investigated in a quasi-one-dimensional approximation. The radial propagation of the turbulent front is represented as a prescribed entrainment boundary and the chemical composition of the initial flow entering the boundary is calculated according to existing approximate methods for tracing chemical reactions in laminar flows. In the absence of a suitable chemical kinetics theory for turbulent flows, only the limiting cases of extremely slow and extremely fast viscous dissipation are considered for the subsequent turbulent mixing process. Specific examples are presented for the flow behind hypersonic spheres in air. In the slow-dissipation case, the high-entropy gas in the wake remains hot, and may even be reheated strongly by three-body atomic recombination. This gives rise to large amplitude fluctuations of the chemical species. In the fast dissipation case, the temperature generally falls off rapidly with distance behind the sphere, but moderately strong reheating may still take place due to sudden enhancement of the exothermic exchange reaction $N + O_2 \rightarrow NO + O$. The mean electron density in the far wake is found to be extremely sensitive to the mixing model.

I. Introduction

THE study of wake phenomena behind high-speed objects in the earth's atmosphere has stimulated considerable interest in hypersonics research in recent years.[1] In 1959, Feldman[2] obtained a set of numerical solutions for the conduction-controlled laminar trails behind spheres at hypersonic speeds, using a quasi-equilibrium equation of state for the high-temperature air throughout the flow field. However, from an earlier estimate, by one of the authors,[3] of the characteristic chemical and ionization relaxation times for the various parts of the flow field, it was found that the high-entropy wake[4] would always be out of chemical equilibrium except at gas densities corresponding to hypersonic flight at relatively low altitudes. In view of the fact that the wake behind objects of ordinary sizes would become turbulent at low altitudes, the assumptions of laminar flow and of local chemical equilibrium did not appear to be mutually compatible. This, indeed, has been found to be the case from more detailed calculations of the streamwise relaxation histories[5] and from recent experimental studies of the wake transition phenomenon.[6–10]

The theoretical problem of turbulent diffusion in the wake of a blunt-nosed body at hypersonic speeds was first treated by Lees and Hromas[11] in 1961, adopting Reynolds hypothesis of similarity between the turbulent transfer of mass, momentum and energy, and using a turbulent diffusivity extrapolated from Townsend's low-speed experiments. In order to bring out the main fluid dynamics effects without undue complications by rate processes, Lees and Hromas again assumed the equation of state of the gas to be that corresponding to local thermodynamic equilibrium everywhere in the flow field. This treatment has also been extended to wakes behind slender hypersonic objects, such as hemisphere cones and pure cones.[12] Although the calculated rate of growth of the turbulent wake appeared to agree well with experimental observations, predictions of the thermal and chemical properties of the wake from such theoretical models remain of doubtful value until the question of reaction rates in the flow field is properly examined.

More recently, various authors[13–15] have proposed to use the integral method[4] for simultaneous treatment of diffusion and chemical relaxation in turbulent as well as laminar wakes behind objects of arbitrary (but axisymmetric) shape. The terms for production (or depletion) of chemical species in the species conservation equations in these treatments are

Presented as Preprint 63-449 at the AIAA Conference on Physics of Entry into Planetary Atmospheres, Cambridge, Mass., August 26–28, 1963; revision received April 27, 1964. This work was supported jointly by Headquarters, Ballistic Systems Division, Air Force Systems Command, U. S. Air Force, under Contract No. AF 04(694)-33 and Advanced Research Projects Agency monitored by Army Missile Command, U. S. Army, under Contract No. DA-19-020-AMC-0210 as part of Project Defender. The authors wish to acknowledge the help and encouragement from many of their colleagues at the Avco-Everett Research Laboratory during the course of this work. They wish to thank especially J. D. Teare for his invaluable advice, and G. J. Dreiss for his able assistance in carrying out the computer program required for the numerical calculations.

* Principal Research Scientist. Associate Fellow Member AIAA.
† Principal Research Scientist.

considered identical in form for both the laminar and the turbulent cases, and the reaction rate constants employed in subsequent numerical calculations are often those published in the literature for homogeneous gas mixtures. Such treatment of chemical reactions in turbulent flow is difficult to justify since the instantaneous reaction rates within any volume element of a chemically active, turbulent fluid with initial large-scale inhomogeneities are expected to be highly sensitive to the degree of microscopic mixing among the different chemical species originated from different parts of the flow field.

In the present paper, the problem of chemical reactions in the turbulent wakes of hypersonic objects is treated from a chemicophysics point of view, with a special objective of gaining some insight into the primary effects of interaction between the turbulent motion and the relaxation processes in a nonequilibrium flow field. To do this, we shall adopt a simple quasi-one-dimensional model in which the rate of growth of the turbulent boundary with axial distance x behind the object is assumed known, and all mean properties within such a boundary are assumed to be functions of x alone. The initial state of the gas entering the entrainment boundary is to be determined from one of the existing approximate methods for following chemical reactions in laminar flow fields. In the absence of suitable chemical kinetics theory for heterogeneous turbulent flows, only two extreme models of turbulent mixing, which allow simple application of "laminar" chemical kinetics, will be considered.

II. Two Extreme Models of Turbulent Mixing

Restricting our attention to the consideration of only axially symmetric flow, the present treatment starts with a replacement of the actual fluctuating boundary of the apparently turbulent wake by a smoothed-out time-averaged boundary $y_f(x)$. We shall assume that the flow everywhere outside this boundary is laminar and steady in a coordinate system fixed with the body, and that the mean flow inside the boundary is quasi-one-dimensional. Since the rate of radial propagation of the turbulent front is generally much greater than the rate of propagation of viscous effects by molecular diffusion, it is reasonable to neglect all effects of viscosity and molecular diffusion in the external flow. At flight velocities much below meteoric velocities, one may also neglect radiative heat loss from the wake.

The smoothed-out boundary $y_f(x)$ is to be determined either directly from experimental observations,[8] or from an approximate theory, such as the one proposed by Lees and Hromas.[11] With this boundary already specified, the problem of mixing and chemical reactions within the turbulent zone becomes one of adiabatic quasi-one-dimensional channel flow with mass injection at the boundary. The chemical state of the gas at the boundary is taken to be identical to that at the corresponding geometrical point in a purely laminar, inviscid, but chemical reacting flow field behind the same object.

To determine the subsequent reactions and mean flow properties within the quasi-one-dimensional wake as a function of axial distance x, the following two extreme models of mixing are employed:

A. Inviscid Random Convection

This model assumes that the eddy motion simply stirs up and redistributes the initial large-scale inhomogeneities across the wake in a somewhat random manner without molecular diffusion and viscous dissipation across the "grain boundaries" of the eddies. This corresponds to the case of random convection discussed by Obukhoff,[16] Corrsin,[17] and Batchelor[18] in the limit of zero viscous dissipation rate. It has also been called the "marble cake" model by Herlin, Herrmann and others[19, 20] in interpreting the apparently large density fluctuations observed by Slattery and Clay in some recent ballistic range experiments.[21] Since the time histories for the individual fluid elements are not disturbed by the convective motion according to this model, the mean flow properties across the wake are simply given by the arithmetical averages of the corresponding flow variables in an equivalent inviscid laminar flow over the same width of the wake. Similarly, the mean-square deviations of the various flow properties about the mean can be obtained from similar averaging of the radial distributions of the corresponding quantities in the equivalent laminar flow.

B. Homogeneous Mixing

This model assumes that the new fluid crossing the turbulent boundary is instantaneously and thoroughly mixed with the old fluid already within the boundary at any axial distance x. For this extreme model, which represents the limiting case of infinitely fast viscous dissipation, the mean flow properties across the wake as a function of x can be obtained from a simultaneous tracing of the mixing and reaction histories at the local mean temperature and density so determined.

From elementary considerations, one may expect the first model to be a good approximation to the early part of the turbulent wake near the object, especially at high Reynolds number. This is because of the rapid development of shear instability in the transition process,[22] so that the rate of turbulence production generally overwhelms the rate of viscous dissipation. Although the direct applicability of the second model to any part of the wake is not clear at this time, it does nevertheless serve as a useful reference for the study of the possible effects of extremely rapid mixing and dissipation.

III. Example of Blunt-Body Wake Flow

In order to bring out the principal effects of different mixing models on the chemical reactions in a flow field with large scale initial inhomogeneities, we shall consider the example of flow behind spheres or sphere-like blunt objects at hypersonic speeds through the earth's atmosphere.

A. Mapping of the Chemically-Reacting Inviscid Flow Field

The chemically-reacting, laminar, inviscid flow field around a hypersonic object of arbitrary shape can be obtained from a number of approximate methods.[5, 23–27] For mapping of the high-entropy flow field over great distances behind the object for wake studies, the simplicity of the streamtube method[5, 23, 24] generally outweighs the penalty of possible errors caused by an imprecise prescription of the pressure field. This is especially true for flow over smooth blunt objects where the over-all chemical relaxation history is relatively insensitive to the details of the base flow.

As a specific example, we shall consider an axisymmetric flow associated with a bow shock shape shown in Fig. 1 and a pressure field given in Fig. 2. The analytic curve shown in Fig. 1 is taken from Fig. 11 of Ref. 12 for a hemisphere-cylinder at flight Mach number $M_\infty = 22$, and the experimental points are obtained from a typical ballistic range schlieren photograph taken at the Avco-Everett Research Laboratory of a 0.22-in.-diam spherical pellet at 15,000 fps velocity in room temperature air at 76 mm Hg pressure. The streamwise pressure distribution along typical streamlines behind the shock shown in Fig. 2 is obtained from a smooth fit between the Newtonian distribution[4] in the subsonic region and the second-order blast wave distribution[28, 29] in the supersonic region for flow over a sphere at $M_\infty = 20$. Note that all perturbations caused by details of the base flow (e.g., over-expansion, separated flow, recompression shock, etc.[2, 11]) have been smoothed out so that the resultant pressure

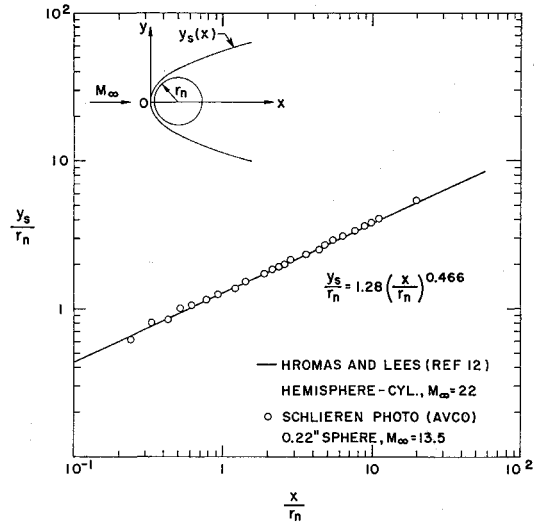

Fig. 1 Bow shock shape for hypersonic air flow over a sphere of radius r_n. y_s is the radial coordinate of the shock, and x is the axial distance measured from the shock apex.

distribution is more representative of the flow over a sphere with suitably streamlined afterbody rather than the flow over a pure sphere. Such a smoothed-out process undoubtedly introduces some ambiguity in the interpretation of numerical results, but the ambiguity is expected to be confined only to the near wake (i.e., small axial distances behind the object).

Considering air to be a pure mixture of O_2 and N_2 in the ratio 21/79 by partial pressure, and using reaction rate constants summarized in Refs. 30 and 31, the inviscid flow field has been mapped out according to the streamtube method to an axial distance of several thousand times the sphere radius r_n for several values of r_n over a wide range of ambient air density ρ_∞. To reduce the number of flow variables to a minimum, we have fixed the flight velocity U_∞ to a value of 22,000 fps. This is not a serious limitation since, within certain limits, the characteristic relaxation distances of interest are not very sensitive functions of shock strength.[3, 31] Furthermore, there actually exists some close resemblance between the relaxation histories of different streamlines originating from different parts of the bow shock of different objects, provided that the starting shock strength is the same (i.e., same normal velocity component entering the shock). Therefore, the general conclusions obtained from the present investigation can be extrapolated to some extent to other flight velocities.

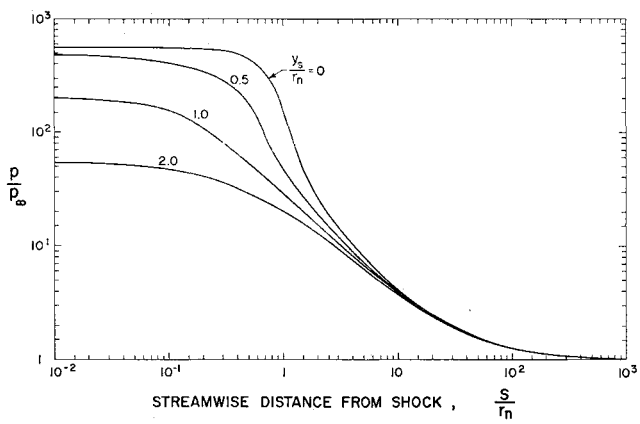

Fig. 2 Streamwise pressure distribution employed in reacting inviscid flow calculations. This hypothetical distribution is approximately that for hypersonic air flow over a sphere of radius r_n (with suitably streamlined afterbody) at $M_\infty = 20$. S is the streamwise distance measured from the bow shock surface along streamlines that intersect the shock at the various indicated values of y_s/r_n.

The general complexity of the chemical and ionization relaxation histories in the inviscid flow fields of blunt objects is illustrated by the typical plots of temperature, atom concentration, and electron density profiles in Figs. 3a–3d. These profiles, plotted against the streamtube ordinate y_s/r_n, are taken at 100 radii behind a sphere of 1-ft radius at ambient air densities corresponding to the various indicated altitude in an Air Research and Development Command Model Atmosphere[32] (y_s is the radial distance at which the streamtube intersects the bow shock). From this specific example, it is quite clear that the quasi-equilibrium flow assumption[2, 3, 11, 12] has, indeed, a very limited range of validity for the treatment of hypersonic wake flow in the atmosphere. In fact, even at an altitude of 50,000 ft, there still exists a noticeable portion of the high-entropy flow field (i.e., $1 < y_s/r_n < 2$) which is out of chemical equilibrium. For objects of smaller than 1-ft dimensions, the nonequilibrium zone would spread further inward toward the axis and persist to lower altitudes.

From the wide divergence in shape of the various inviscid profiles illustrated in Figs. 3a–3d, it is quite clear that extreme care must be exercised in the selection of functional forms for the analytical profiles to be employed in any laminar diffusion calculation using the integral method.[13–15] In the case of turbulent flow, the existence of such complicated external profiles may also be expected to contribute significantly to the difficulty in any two-dimensional treatment of the wake.

B. Scaling of Binary and Ternary Reactions

Roughly speaking, for a simple hypersonic flow field consisting of one main shock compression (subsonic) region followed by an expansion (supersonic) region, as the one under consideration, the chemical and ionic reactions along each streamtube could get out of equilibrium in three different ways: 1) the endothermic reactions (e.g., dissociation and ionization) lag behind the shock compression process all the way up to the sonic point; the exothermic reactions (e.g., atom-atom and electron-ion recombinations, electron attachment, etc.) also lag behind the subsequent expansion; 2) the endothermic reactions catch up with the shock compression process before reaching the sonic point, but the exothermic reactions lag behind the subsequent expansion; 3) the endothermic reactions lag behind the shock compression process up to the sonic point, but the exothermic reactions keep pace with the subsequent expansion process. Because most of the endothermic reactions of interest are binary, whereas some of the important exothermic reactions are ternary,[30, 31] all of the preceding three situations could prevail, depending on the particular combination of r_n and ρ_∞. The problem of scaling of the inviscid flow field chemistry, therefore, becomes extremely complicated, if at all possible. However, it can be shown[33] that situation 3 actually would not occur except for objects of microscopic size at densities greater than the normal sea level density ρ_0. Furthermore, even though perfect scaling of the entire flow field is not possible, there exists some distinct regions in the r_n vs ρ_∞/ρ_0 plane where either binary scaling,[31, 34] or a simple combination of binary and ternary scaling,[33] would be adequate for many aspects of the wake flow problem.

For the present treatment of the quasi-one-dimensional turbulent wake, the approximate boundaries for these scaling regions are illustrated in Fig. 4. The laminar-turbulent transition boundary located at $(\rho_\infty/\rho_0)r_n = 10^{-4}$ ft corresponds to the blunt-body critical Reynolds number suggested by Lees in Ref. 10. At the flight velocity under consideration, this boundary happens to coincide approximately with the boundary dividing situations 1 and 2 described in the

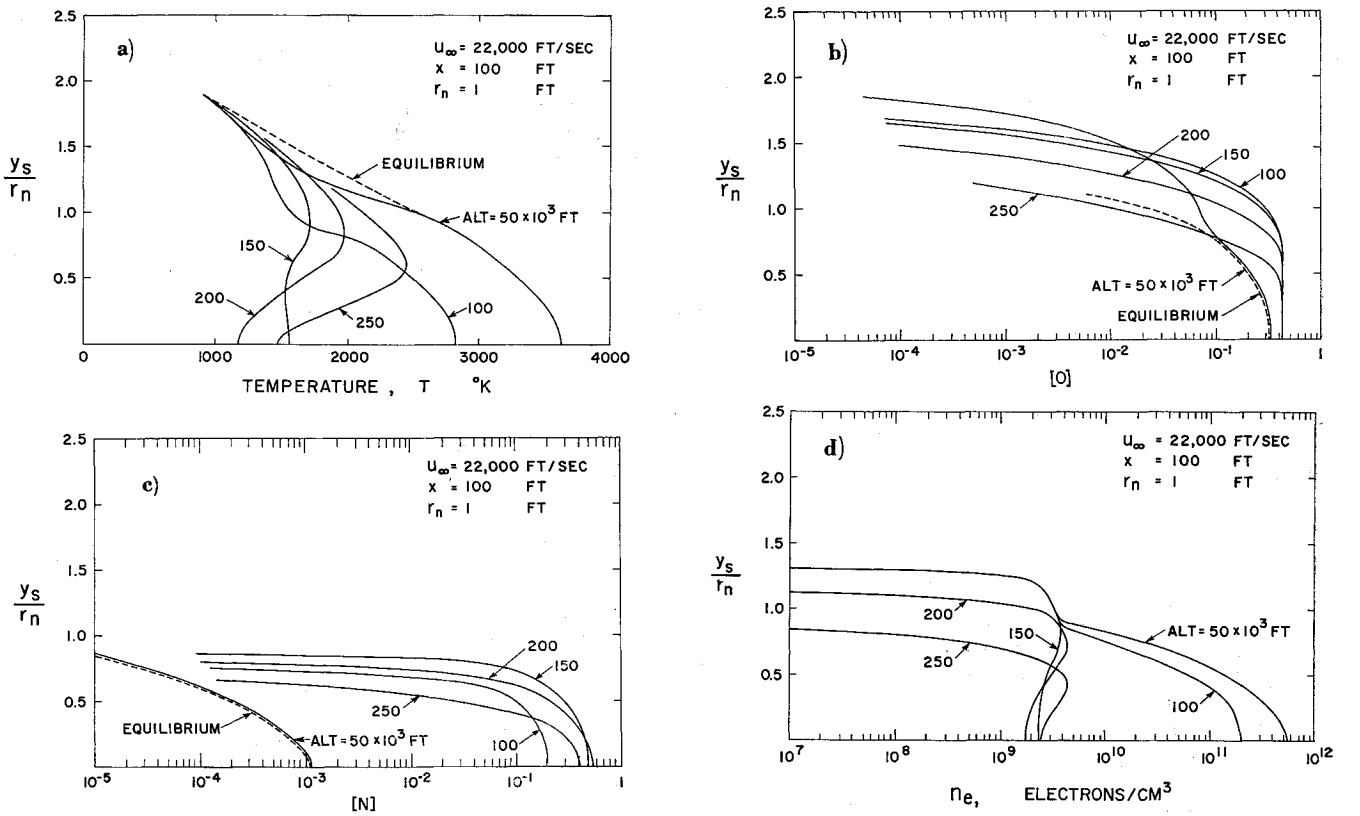

Fig. 3 Typical radial distributions of temperature, atom concentration ([O] denotes number of moles of O atoms per original mole of air, etc.) and electron density for axisymmetric laminar, inviscid, but chemically reacting hypersonic air flow over sphere of 1-ft radius at 22,000 fps velocity and at ambient density corresponding to the various indicated altitude (Air Research and Development Command 1959 Model Atmosphere). The example depicted is for an axial distance of 100 ft behind the shock. Note that the radial distributions are plotted against the streamtube coordinate y_s/r_n, which refers to the location of the streamtube at the bow shock. The dotted curves for quasi-equilibrium flow are based on ambient air density corresponding to a referenced altitude of 50,000 ft.

preceding paragraph. The boundary $(\rho_\infty/\rho_0)^2 r_n = 10^{-5}$ ft between the binary scaling region B and the binary-ternary scaling region B-T is determined by the criterion that three-body atomic recombination recovers only about 10% of the total energy invested in dissociation per unit mass flow across the entire inviscid flow field at a distance of 100 radii behind the object. The boundary $(\rho_\infty/\rho_0)^2 r_n = 4 \times 10^{-2}$ ft between region B-T and the equilibrium region E marks the point at which the neglect of all nonequilibrium effects would only cause an error of 10% in the calculation of total static enthalpy per unit mass flow across the inviscid flow field at the same axial distance. Within region B, all objects with the same value of $(\rho_\infty/\rho_0)r_n$ have approximately the same distributions of temperature, chemical, and ionic species (in mole fraction) in a flow field plotted in terms of the non-dimensional coordinates x/r_n and y/r_n. Within region B-T, all objects with the same value of $(\rho_\infty/\rho_0)^2 r_n$ have similar distributions of temperature and chemical species but not necessarily of the electrons and ions. The reason is that although the rate-limiting step for the chemical relaxation processes in the supersonic part of the flow field is three-body atomic recombination, the rate-limiting step for the ionic relaxation processes is predominantly two-body electron-ion recombination.[31] Therefore, unless the latter reaction is sufficiently rapid to keep the ionic species in quasi-equilibrium with the local chemical composition and temperature, the distribution of electrons and ions in the flow field will not scale simply with the ternary scaling parameter $(\rho_\infty/\rho_0)^2 r_n$. The ionic relaxation histories, however, do not have any significant influence on the chemical relaxation histories since the degree of ionization is generally quite small in the hypersonic flow field.[31]

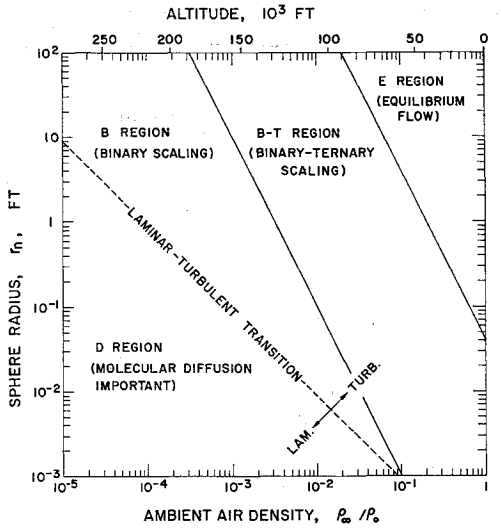

Fig. 4 Approximate boundaries for scaling of chemically reacting hypersonic flow field behind spheres at 22,000 fps velocity in air.

C. Location of the Turbulent Front

The rate of growth of the turbulent front behind spheres at hypersonic speeds has been studied experimentally by Slattery and Clay,[8] and theoretically by Lees and Hromas.[10,11] For small distances behind the sphere, Lees and Hromas predicted that the initial width as well as the rate of growth of the turbulent front would be controlled by skin friction and by detail structure of the based flow, and hence would

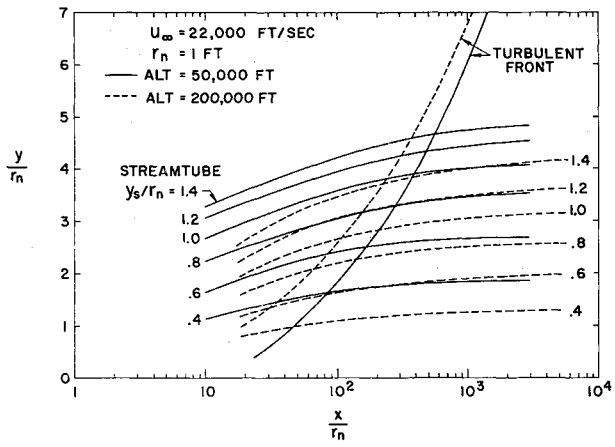

Fig. 5 Typical location of turbulent front in relation to locations of inviscid laminar streamtubes behind a sphere of 1-ft radius at 22,000 fps velocity and at two different altitudes.

be Reynolds number dependent. This was consistent with the trend of Slattery and Clay's data, even though there existed considerable scatter in the experimental data for the first 100 diam behind the sphere. At greater axial distances, however, both theory and experiment indicated that the width of the turbulent wake grew quite clearly with the cube-root of the axial distance and became insensitive to Reynolds number. For the present problem, we have adopted the following simple analytic expression for the turbulent entrainment boundary:

$$y_f/r_n = 18Re_\infty^{-1/4} + 0.8[(x/r_n)^{1/3} - 20^{1/3}] \text{ for } x/r_n \geq 20 \quad (1)$$

where

$$Re_\infty \equiv \rho_\infty U_\infty r_n/\mu_\infty \cong 10^7 M_\infty(\rho_\infty/\rho_0)r_n$$

is the Reynolds number based on the ambient condition (r_n given in feet for the last expression).

Such a boundary approximately satisfies the criterion that, at small axial distances (i.e., $x/r_n \leq 20$), the rate of mass flow through the turbulent core is equal to the rate of mass flow into the boundary layer on the surface of the sphere (based on local inviscid flow value of ρu for the core flow). At large axial distances ($x/r_n \gtrsim 100$), Eq. (1) fits closely the experimental points summarized by Lees and Hromas.[11]

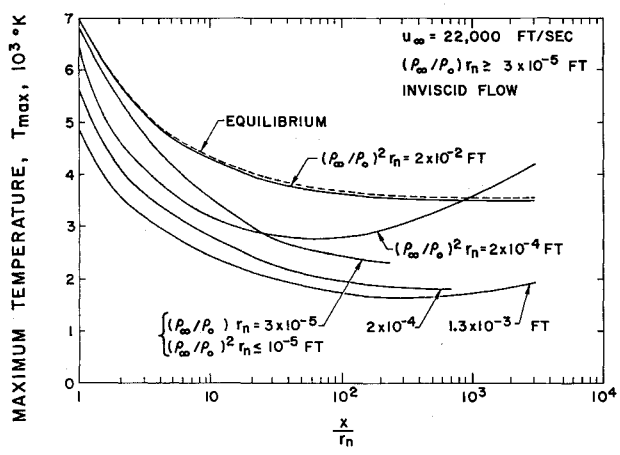

Fig. 6 Maximum local temperature in chemically reacting inviscid flow field behind spheres at 22,000 fps velocity as a function of axial distance and the binary-ternary scaling parameters. Note that the dotted curve for quasi-equilibrium flow is only approximate since the equilibrium solution is slightly dependent on absolute density.

D. The Entrainment Process

The axial distance at which the turbulent front represented by Eq. (1) intersects inviscid streamtubes originating from different parts of the bow shock wave is illustrated in Fig. 5 for a sphere of 1-ft radius at two different altitudes. From the typical profiles shown in Fig. 3, it is seen that the early stage of development of the turbulent wake involves entrainment of the most highly dissociated gas in the flow field. On account of the flatness of the chemical composition profiles for the external flow near the axis, the mean chemical composition within the turbulent front is not much affected by the entrainment process. As the turbulent front grows, the chemical composition of the inviscid flow entering the front changes in the direction of decreasing degree of dissociation at an ever accelerating pace until all the dissociated gas is eventually entrained. The point for essentially complete entrainment of the dissociated gas is located somewhere between 100 and 600 radii behind the sphere, depending upon the combination of radius and air density. The dilution effect of such an entrainment process would tend to shift the averaged chemical composition across the turbulent wake from that typical of the high-entropy gas along the stagnation streamline in an equivalent inviscid laminar flow continuously toward that typical of the cold ambient air (i.e., 21% O_2 + 79% N_2).

E. Mean Properties of the Turbulent Wake Calculated According to the Two Extreme Models of Mixing

1. Inviscid random convection

For the inviscid random connection model, each fluid element is assumed to retain its own identity during the random convection process. Thus, the chemical reactions within each fluid element should proceed exactly the same way as if the flow field were completely laminar. At a given axial distance x, the peak value as well as the volume integral of any physical quantity Φ over a unit length of the turbulent wake would be the same as those given by the equivalent inviscid laminar flow profile out to the radial distance of the turbulent front $y_f(x)$. The radial distribution of Φ, however, is randomized by the convective motion within $y_f(x)$. Because of the invariance of the volume integral of Φ with respect to its radial distribution, the averaged value of Φ across the turbulent wake is simply given by

$$\langle\Phi\rangle = \frac{2}{y_f(x)}\int_0^{y_f(x)} \Phi_i(x, y)y\,dy \quad (2)$$

where $\Phi_i(x, y)$ is the distribution of Φ in the equivalent inviscid laminar flow. Similarly, the mean-square deviation of Φ about its averaged value within the turbulent front is given by

$$\langle|\Phi - \langle\Phi\rangle|^2\rangle = \frac{2}{y_f^2(x)}\int_0^{y_f(x)} |\Phi_i(x, y) - \langle\Phi\rangle|^2 y\,dy \quad (3)$$

Typical plots of the peak temperature T_{max}, the averaged electron number density $\langle n_e\rangle$, and the root-mean-square deviations of mass density and of electron density within the turbulent wake thus obtained are shown in Figs. 6–8 as functions of the normalized axial distance x/r_n and the scaling parameters $(\rho_\infty/\rho_0)r_n$, $(\rho_\infty/\rho_0)^2 r_n$. It is interesting to note that, according to this extreme model, there exists an anomolous reheating effect in the *B-T* region of Fig. 4 because of delayed three-body atomic recombination of the high-entropy gas in an expanding flow field, causing the peak temperature to rise above that corresponding to isentropic quasi-equilibrium flow at some large distances behind the object. Because of the persistency of fairly high temperature within each volume element of ionized gas into the far wake, electron attachment[3] is completely inhibited. This leads to the persistency of relatively high averaged electron density out to very large values of x/r_n (see Fig. 7).

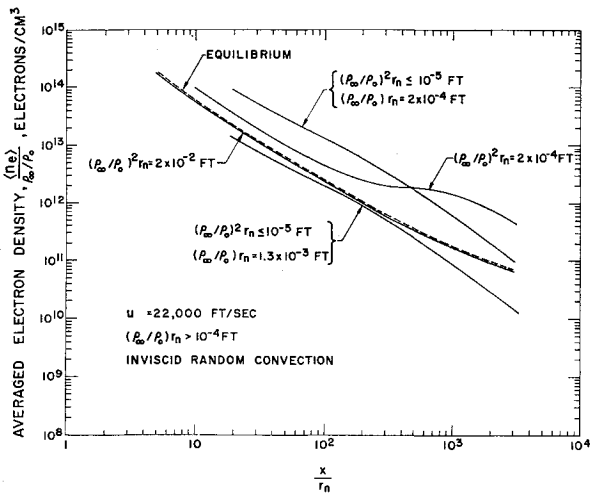

Fig. 7 Averaged electron number density within turbulent wake behind spheres at 22,000 fps velocity as a function of axial distance and the binary-ternary scaling parameters (inviscid random convection model). Note that scaling of electron density in *B-T* region of Fig. 4 is only approximate since it is neither in quasi-equilibrium with the local chemical composition, nor completely recombination-controlled.

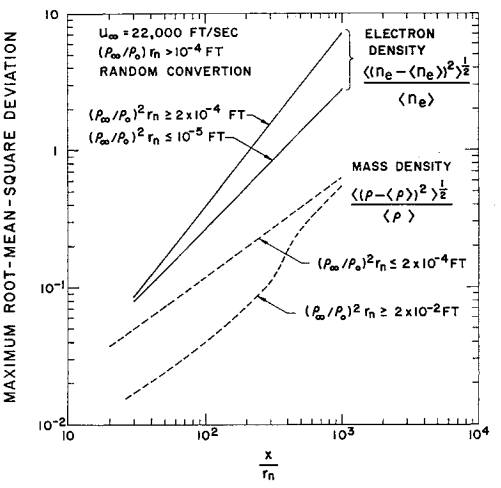

Fig. 8 Root-mean-square deviation of mass density and of electron number density within turbulent wake calculated according to the inviscid random convection model. This represents maximum possible degree of inhomogeneity in the wake since any diffusion effect would tend to smooth out the gradients and hence decrease the averaged fluctuations. Example depicted is for spheres at 22,000 fps in air.

The present extreme model also predicts very large root-mean-square deviations of the mass density and of the electron density about their respective average values in the turbulent wake (see Fig. 8). In fact, the ratio between the root-mean-square deviation and the averaged value of these two quantities at very large axial distances is to increase indefinitely with $(x/r_n)^{2/3}$. This, of course, cannot happen in practice, since the continued increase in averaged gradient caused by the random convection process is ultimately checked by molecular diffusion.[18] The maximum axial distance up to which the root-mean-square deviation of any physical quantity may follow the upper-bound value represented by Eq. (3) is expected to be governed by the actual viscous dissipation rate in the turbulent wake.

2. *Homogeneous mixing*

For the homogeneous mixing model, the newly entrained gas is assumed to be instantaneously and homogeneously mixed with the old, so that chemical reactions should proceed according to the local temperature and chemical composition at any given axial distance x. Thus, the rate of change of the mean number density $\bar{n}_\zeta$ of a chemical or ionic species of type ζ in the wake with axial distance is determined by the ordinary differential equation that follows:

$$\frac{d}{dx}(\bar{n}_\zeta \bar{u} y_f^2) = n_{\zeta i} u_i \frac{d}{dx}(y_f^2) + y_f^2 \left(\frac{d\bar{n}_\zeta}{dt}\right)_c \qquad (4)$$

where $(d\bar{n}_\zeta/dt)_c$ is the net time rate of change of $\bar{n}_\zeta$ due to all chemical and ionic reactions within the wake, which can be expressed explicitly as a sum of terms involving the product of the rate constant and the local concentrations of the reactants.[31] These species equations (one for each species) can be solved, at least by numerical methods, together with the conservation equations for mass, momentum, and energy for the steady quasi-one-dimensional flow:

$$(d/dx)(\bar{\rho}\bar{u}y_f^2) = \rho_i u_i (d/dx)(y_f^2) \qquad (5)$$

$$(d/dx)(\bar{\rho}\bar{u}^2 y_f^2) = \rho_i u_i^2 (d/dx)(y_f^2) - y_f^2 (d\bar{p}/dx) \qquad (6)$$

$$\bar{h} + (\bar{u}^2/2) = h_\infty + (u_\infty^2/2) \qquad (7)$$

In the preceding equations, ρ, u, p, and h denote, respectively, the mass density, axial velocity, pressure, and specific enthalpy (including chemical energy) per unit mass of the gas mixture; barred quantities refer to mean value within the turbulent wake; subscript i refers to the local inviscid flow condition just outside of the turbulent front y_f; and subscript ∞ refers to the ambient air condition. It may be pointed out that the problem is now somewhat over-determined in the sense that the mean pressure $\bar{p}$ calculated from a simultaneous solution of Eqs. (4–7), according to the prescribed entrainment boundary y_f, may not come out the same as the pressure distribution originally used in the inviscid laminar flow calculations. Such a mismatch in pressure, however, has been found to be slight enough to be negligible, especially in view of the general insensitivity of the chemical relaxation histories to perturbations in flow field pressure distribution.[25]

The mean temperature and the mean axial velocity within the turbulent wake calculated according to this model are shown in Figs. 9 and 10. The mean electron number density is plotted in Fig. 11 for the case of no attachment (high altitude limit). In Fig. 12, the mean electron density calculated with the effect of attachment included for the special case of a 1-ft sphere is plotted (dotted curves) for comparison with that corresponding to the other extreme model shown in Fig. 7 (solid curves).

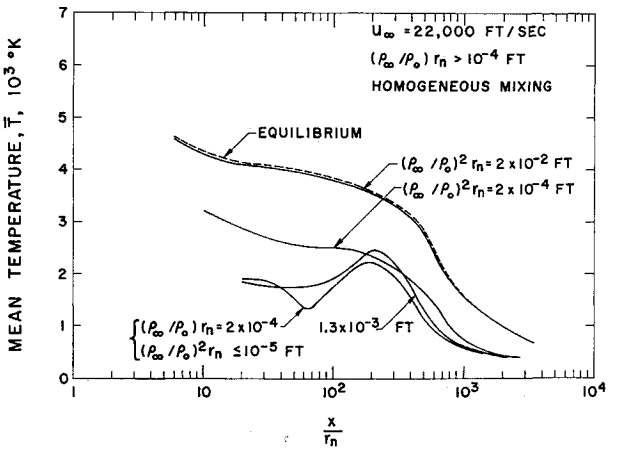

Fig. 9 Mean temperature within turbulent wake behind spheres at 22,000 fps velocity as a function of axial distance and the binary-ternary scaling parameters (homogeneous mixing model).

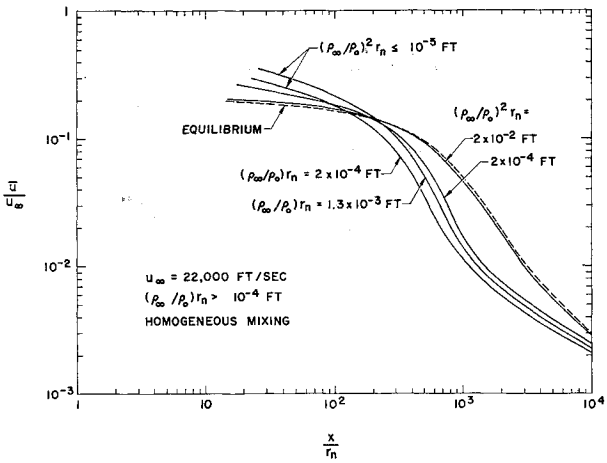

Fig. 10 Mean axial flow velocity within turbulent wake behind spheres at 22,000 fps velocity as a function of axial distance and the binary-ternary scaling parameters (homogeneous mixing model).

Comparison of Figs. 9 and 6 shows that the mean temperature in the homogeneously mixed wake first roughly follows the peak temperature in the equivalent inviscid laminar flow for some distance until the dilution effect of entrainment comes into play. For values of $(\rho_\infty/\rho_0)^2 r_n$ lying in the *B-T* region of Fig. 4, the mean temperature appears to fall monotonically with axial distance, indicating that the rate of reheating due to delayed three-body atomic recombination cannot keep pace with the rate of dilution. However, in the *B* region of Fig. 4, where most of the dissociation energy in the high-entropy gas is initially frozen out, there exists a fairly strong reheating effect starting at about $x/r_n = 50$. This is caused by a sudden enhancement of the exothermic chain reactions:

$$N + O_2 \rightarrow NO + O \tag{8}$$

$$N + NO \rightarrow N_2 + O \tag{9}$$

when additional O_2 molecules are entrained into the wake from the lower enthalpy external flow. To a somewhat smaller extent, enhancement of reaction (9) due to entrainment of additional NO molecules from the external flow also contributes to the wake reheating effect. Such a reheating process may be expected to continue until most of the N atoms in the wake are converted into O atoms by reactions (8) and (9).

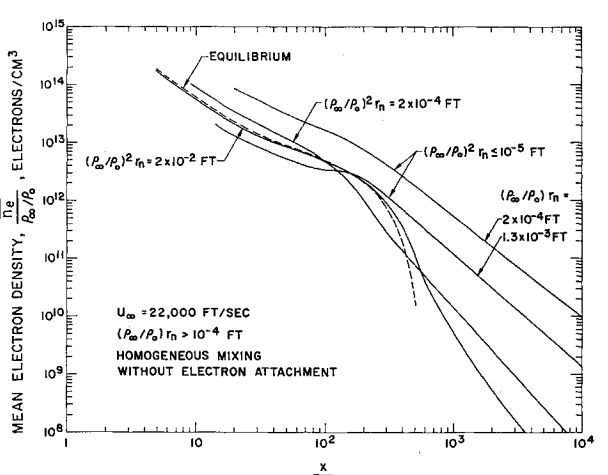

Fig. 11 Mean electron number density within turbulent wake behind spheres at 22,000 fps velocity as a function of axial distance and the binary-ternary scaling parameters (homogeneous mixing model). Since the mean electron density does not scale exactly with $(\rho_\infty/\rho_0)^2 r_n$ in the *B-T* region of Fig. 4, the two curves for $(\rho_\infty/\rho_0)^2 r_n = 2 \times 10^{-4}$ and 2×10^{-2} ft are only meant to be representative for spheres of radii not drastically different from the reference value of 1 ft. The effect of electron attachment is not shown in this plot.

Comparing the mean electron density $\bar{n}_e$ shown in Fig. 11 with the averaged electron density $\langle n_e \rangle$ shown in Fig. 7, it is seen that these two quantities assume approximately the same value during the early phase of the entrainment process $(x/r_n \lesssim 50)$. When the dilution effect of entrainment comes into play at larger values of x/r_n, the mean electron density $\bar{n}_e$ falls off more rapidly with axial distance than $\langle n_e \rangle$. The difference between the two becomes more marked at high air densities (or low altitudes) where the mean electron density tends toward quasi-equilibrium with the local N and O atom concentrations at the local temperature. At low densities or high altitudes) the local electron density is controlled by the binary dissociative recombination processes, such that, in the absence of electron attachment,

$$\left(\frac{d\bar{n}_e}{dt}\right)_c \cong -\bar{n}_e \sum_{\zeta'} \kappa_{e\zeta'}(\bar{T})\bar{n}_{\zeta'} \tag{10}$$

Since the recombination rate constant $\kappa_{e\zeta'}(\bar{T})$ is only weakly temperature dependent,[31] the difference between $\bar{n}_e$ and $\langle n_e \rangle$ becomes small. However, it may be noted that the electron density generally falls off somewhat more rapidly than the inversed first power of x. (The asymptotic behavior $\bar{n}_e \sim x^{-1}$ discussed in Refs. 5 and 10 corresponded only to the situation where $\kappa_{e\zeta'}$ = constant.)

Because the mean temperature $\bar{T}$ as a function of x/r_n can be scaled according to either $(\rho_\infty/\rho_0)r_n$ or $(\rho_\infty/\rho_0)^2 r_n$ in the *B* or *B-T* regions of Fig. 4, respectively, Eqs. (4) and (10) suggest that the product $\bar{n}_e r_n$ as a function of x/r_n can be scaled according to the same parameters, as long as the electrons and ions are far out of equilibrium with the local atom concentrations and temperature. In Figs. 7 and 11, the preceding scaling law was found to hold only in the *B* region and in the lower part of the *B-T* region of Fig. 4 (i.e., small r_n). In the upper part of the B-T region (i.e., large r_n) the electrons and ions tend to be in quasi-equilibrium with the local atom concentrations and temperature so that the quantity $\bar{n}_e/(\rho_\infty/\rho_0)$ can be scaled according to the parameter $(\rho_\infty/\rho_0)^2 r_n$. In the in-between region where the electrons and ions are neither in quasi-equilibrium nor sufficiently far away from equilibrium with respect to the local atom concentrations and temperature, no simple scaling between r_n and (ρ_∞/ρ_0) is possible. For this reason, the curves labeled $(\rho_\infty/\rho_0)^2 r_n = 2 \times 10^{-2}$ ft and $(\rho_\infty/\rho_0)^2 r_n = 2 \times 10^{-4}$ ft in Figs. 7 and 11 are only meant to be representative curves for typical sphere radii of the order of 1 ft. These should not be used for scaling to values of r_n which are drastically different from the referenced 1-ft value. Further discussion of this scaling problem and illustration of additional numerical examples are out of the scope of the present paper, but may be found in a separate report by the authors.[33]

The mean electron density curves with electron attachment shown in Fig. 12 (dotted curves) were calculated from the three-body attachment coefficient κ_a by Biondi, et al.[35, 36] for the process

$$O_2 + O_2 + e \underset{\kappa_d}{\overset{\kappa_a}{\rightleftharpoons}} O_2^- + O_2 \tag{11}$$

using a binding energy of 0.46 ev as suggested by Phelps and Pack.[37] It was found that, in order for the attachment process to affect the mean electron density distribution in the far wake, two separate conditions must be simultaneously satisfied[3]: 1) the mean temperature must fall below a critical value of approximately 600°K; and 2) the air density must be sufficiently high so that the characteristic attachment time $(\bar{\kappa}_a \bar{n}_{O_2}^2)^{-1}$ becomes comparable to or smaller than the

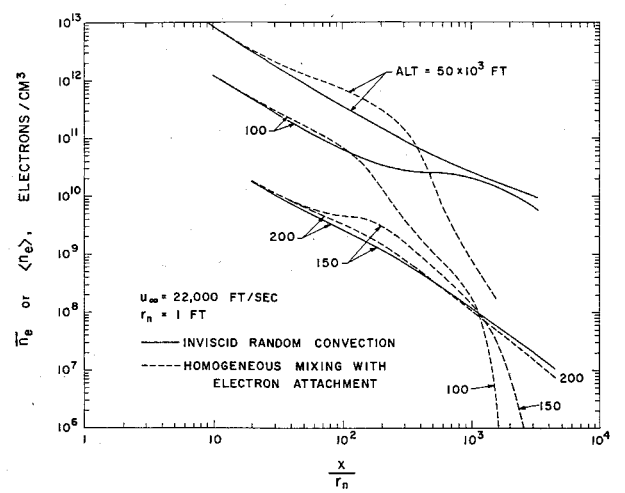

Fig. 12 Comparison of mean and averaged electron densities obtained from the two extreme models of mixing for the turbulent wake behind a sphere of 1-ft radius at 22,000 fps velocity. Electron attachment is included in the homogeneously-mixed model, but its effect appears to be important only for $x/r_n > 10^3$ and at altitudes below about 150,000 ft.

characteristic electron-ion recombination time $(\overline{k_{e\xi}\tilde{n}_e})^{-1}$. For the homogeneously mixed turbulent wake behind spheres, condition 1 is satisfied only for $x/r_n \gtrsim 10^3$. Condition 2 is satisfied when $\rho_\infty/\rho_0 \gtrsim 10^{-3}$. The onset of attachment generally makes the departure of the mean and averaged electron densities calculated according to the two extreme models more drastic (see Fig. 12).

IV. Discussion

The general complexity of the problem of turbulent flow behind hypersonic objects is well demonstrated by the preceding example of the flow behind an object of the simplest possible shape, namely, a sphere. Even though the problem is basically three-dimensional in nature, the present quasi-one-dimensional treatment does allow one to gain some insight into the principal effects of turbulent mixing on the over-all chemical relaxation history in the hypersonic wake. This simple treatment also allows one to make quantitative calculations of those physical properties of the wake which are not sensitive to the mixing model, and to make upper and lower bound estimates of some of the physical properties of the wake which are sensitive to the mixing model.

Notable examples of wake properties that are not very sensitive to the mixing model are the quantities related to the three constancies of motion in adiabatic steady flow (namely, the average mass density, flow velocity, and specific enthalpy). Typical examples of properties that are quite sensitive to the mixing model, but the upper and lower bounds of which can perhaps be estimated, are the mean number densities of all the active chemical and ionic species in the wake (assuming that all the relevant rate constants are known).

The present investigation of finite reaction rates in the turbulent wake clearly shows that, regardless of the mixing model, the assumption of quasi-equilibrium flow is generally a poor one for calculations of wake temperature and of all chemicophysics properties of the wake, except when the combination of object size and air density happens to fall in the E region of Fig. 4. It is also quite clear that indiscriminate application of "laminar" chemical kinetics to turbulent flow can lead to serious errors.

In addition to the mean or averaged properties, there are, of course, various statistical properties of the turbulent wake that are of great practical interest. Even though the present one-dimensional treatment does not concern itself with the statistical problem, some of the general results obtained from this treatment, however, can be used to determine the upper bound for some of the statistical properties. An example of this is the maximum root-mean-square deviation of mass density and of electron number density illustrated in Fig. 8. More quantitative information on such properties can be obtained by suitable consideration of the effect of finite dissipation rate in the turbulent wake flow.

References

[1] Cheng, H. K., "Recent advances in hypersonic flow research," AIAA J. 1, 295–310 (1963).

[2] Feldman, S., "On trails of axi-symmetric hypersonic blunt bodies flying through the atmosphere," Avco-Everett Research Lab. Research Rept. 82 (December 1959); also J. Aerospace Sci. 28, 433–448 (1961).

[3] Lin, S. C., "Ionized wakes of hypersonic objects," Avco-Everett Research Lab. Res. Rept. 151 (June 1959).

[4] Hayes, W. D. and Probstein, R. F., *Hypersonic Flow Theory* (Academic Press Inc., New York, 1959), Chaps. I and VIII.

[5] Lin, S. C. and Teare, J. D., "A streamtube approximation for calculation of reaction rates in the inviscid flow field of hypersonic objects," *Proceedings of the 6th Symposium on Ballistic Missile and Aerospace Technology*, edited by C. T. Morrow, L. D. Ely, and M. R. Smith (Academic Press Inc., New York, 1961), Vol. IV, pp. 35–50.

[6] Hidalgo, H., Taylor, R. L., and Keck, J. C., "Transition in the viscous wakes of blunt bodies at hypersonic speeds," J. Aerospace Sci. 29, 1306–1315 (1962).

[7] Demetriades, A. and Gold, H., "Transition to turbulence in the hypersonic wake of blunt-bluff bodies," ARS J. 32, 1420–1421 (1962).

[8] Slattery, R. E. and Clay, W. G., "Laminar-turbulent transition and subsequent motion behind hypervelocity spheres," ARS J. 32, 1427–1429 (1962).

[9] Lin. S. C., "Radio echoes from a manned satellite during reentry," J. Geophys. Res. 67, 3851–3870 (1962).

[10] Lees, L., "Hypersonic wakes and trails," ARS Preprint 2662-62 (1962).

[11] Lees, L. and Hromas, L., "Turbulent diffusion in the wake of a blunt-nosed body at hypersonic speeds," Space Technology Labs., Rept. 6110-MU-000, Contract No. AF 04(694)-1 (July 1961); also J. Aerospace Sci. 29, 976–993 (1962).

[12] Hromas, L. and Lees, L., "Effect of nose bluntness on the turbulent hypersonic wake," Space Technology Labs., Rept. 6130-6259-KU-000, Contract AF 04(694)-1 (October 1962).

[13] Bloom, M. H. and Steiger, M. H., "Diffusion and chemical relaxation in free mixing," IAS Paper 63-67 (1963).

[14] Webb, W. H. and Hromas, L. A., "Turbulent diffusion of a reacting gas in the wake of a sharp-nosed body at hypersonic speeds," Space Technology Labs., Rept. 6130-6362-RU000 (April 15, 1963).

[15] Lien, H., Erdos, J. I., and Pallone, A. J., "Nonequilibrium wakes with laminar and turbulent transport," AIAA Preprint 63-447 (1963).

[16] Obukhoff, A. M., "Structure of the temperature field in turbulent flow," Izv. Akad. Nauk SSRR Ser. Geograf. i Geofiz. 13, 58 (1949).

[17] Corrsin, S., "On the spectrum of isotropic temperature fluctuations in an isotropic turbulence," J. Appl. Phys. 22, 469–473 (1951).

[18] Batchelor, G. K., "Small-scale variation of convected quantities like temperature in turbulent fluid," J. Fluid Mech. 5, 113–133 (1959).

[19] Herlin, M. A. and Herrmann, J., "Turbulence model of the wake and radar cross section," Massachusetts Institute of Technology, Lincoln Lab., Semi-Annual Tech. Summary Rept. to the Advanced Research Projects Agency, Sec. II-B, pp .II-4–II-9 (December 1962).

[20] Proudian, A. and Feldman, S., "Some theoretical predictions of mass and electron density oscillations and comparisons with experiment," Heliodyne Corp., Res. Rept. 5 (May 1963).

[21] Slattery, R. E. and Clay, W. G., "The turbulent wake of hypersonic bodies," ARS Preprint 2673-62 (1962).

[22] Greenspan, H. P., "Remarks on shear layer instability, breakdown and transition," IAS 31st Annual Meeting, New York (January 20–23, 1963).

[23] Lick, W., "Inviscid flow of a reacting mixture of gases around a blunt body," Fluid Mech. **7**, 128–144 (1960).

[24] Bloom, M. H. and Steiger, M. H., "Inviscid flow with nonequilibrium molecular dissociation for pressure distributions encountered in hypersonic flight," J. Aerospace Sci. **27**, 821–835 (1960).

[25] Vaglio-Laurin, R. and Bloom, M. H., "Chemical effects in external hypersonic flows," *Progress in Astronautics and Rocketry: Hypersonic Flow Research*, edited by F. R. Riddell (Academic Press Inc., New York, 1962), Vol. 7, pp. 205–254.

[26] Gibson, W. E. and Marrone, P. V., "Correspondence between normal shock and blunt-body flows," Phys. Fluids **5**, 1649–1660 (1962).

[27] Hall, J. G., Eschenroeder, A. Q., and Marrone, P. V., "Blunt-nose inviscid airflows with coupled nonequilibrium processes," J. Aerospace Sci. **29**, 1038–1051 (1962).

[28] Lees, L. and Kubota, T., "Inviscid hypersonic flow over blunt-nosed slender bodies," J. Aerospace Sci. **24**, 195–202 (1957).

[29] Feldman, S., "A numerical comparison between exact and approximate theories of hypersonic inviscid flow past slender blunt-nose bodies," Avco-Everett Research Lab., Res. Rept. 71 (1959).

[30] Wray, K. L., "Chemical kinetics of high temperature air," *Progress in Astronautics and Rocketry: Hypersonic Flow Research*, edited by F. R. Riddell (Academic Press Inc., New York, 1962), Vol. 7, pp. 181–204.

[31] Lin, S. C. and Teare, J. D., "Rate of ionization behind shock waves in air. II. Theoretical interpretation," Phys. of Fluids **6**, 355–375 (1963).

[32] Minzner, R. A., Champion, K. S. W., and Pond, H. L., "The ARDC model atmosphere, 1959," Air Force Surveys in Geophysics, No. 115, AFCRC-TR-59-267, Air Force Cambridge Research Center (August 1959).

[33] Hayes, J. E. and Lin, S. C., "Scaling of binary and ternary reactions in the inviscid flow field of blunt hypersonic objects," Avco-Everett Research Lab. Res. Rept. (to be published).

[34] Gibson, W. E. and Marrone, P. V., "Nonequilibrium scaling criterion for inviscid hypersonic air flows," Cornell Aeronautical Lab. Rept. QM-1626-A-8 (1962).

[35] Biondi, M. A., "Atomic collision processes involving electrons and ions in atmospheric gases," *Chemical Reactions in the Lower and Upper Atmosphere* (Interscience Publishers, Inc., New York, 1961), pp. 353–370.

[36] Chanin, L. M., Phelps, A. V., and Biondi, M. A., "Measurement of the attachment of slow electrons in oxygen," Phys. Rev. Letters **2**, 344–346 (1959).

[37] Phelps, A. V. and Pack, J. L., "Collisional detachment in molecular oxygen," Phys. Rev. Letters **6**, 111–113 (1961).